Design improvements for ammonia-fed SOFC systems through power rating, cascade design and fuel recirculation

Cinti, Giovanni ; Liso, Vincenzo; Simon Araya, Samuel

Published in:
International Journal of Hydrogen Energy

DOI (link to publication from Publisher):
10.1016/j.ijhydene.2023.01.008

Publication date:
2023

Document Version
Publisher's PDF, also known as Version of record

Available online at www.sciencedirect.com

ScienceDirect

journal homepage: www.elsevier.com/locate/he

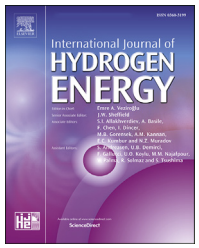

Design improvements for ammonia-fed SOFC systems through power rating, cascade design and fuel recirculation

Giovanni Cinti [a], Vincenzo Liso [b], Samuel Simon Araya [b,*]

[a] Department of Engineering, University of Perugia, Via G. Duranti 93, Perugia, 06125, Italy
[b] AAU Energy, Aalborg University, Pontoppidanstræde 111, Aalborg, 9220, Denmark

HIGHLIGHTS

- Efficiency can be improved using multiple stacks and by recycling the anode gases.
- Heat exchanger area can be reduced by introducing additional stacks to the system.
- Afterburner can be avoided by optimizing the air flow management.

ARTICLE INFO

Article history:
Received 21 October 2022
Received in revised form
22 December 2022
Accepted 1 January 2023
Available online 24 January 2023

Keywords:
SOFC
Ammonia
Fuel cell system
Re-powering
Power rating
Anode off-gas recycling

ABSTRACT

In this paper, design strategies for improving electrical efficiency, thermal design and fuel utilization of an ammonia-fed SOFC are investigated. Three strategies are presented to improve system performances: (i) the introduction of an additional stack to distribute the power i.e. power rating, (ii) the evaluation of the anode off gasses recirculation and (iii) the use of the off gasses to operate a cascade stack (re-powering), where the anode flue gas is recuperated. A system design that integrates these new features is modelled with zero-dimension thermodynamic equations. The three strategies were evaluated for net system efficiency and the heat exchanger area as main design parameters. The power rating allows to reduce the heat exchanger surface while the recirculation and repowering are suitable to increase system efficiency. With an integration of the three solutions, it is possible to achieve an increase in net efficiency from 52.1% to 66% and a reduction in heat exchanger surface area of 67% compared to the reference design that does not consider any of the proposed design strategies.

Introduction

The strong development of renewable energy sources requires improvements in energy management strategies, with a special focus on energy storage solutions. A technology that has been recently gaining interest in literature is the use of ammonia as energy storage solution. The entire concept integrates a power to ammonia technology, to produce green ammonia, and an ammonia to power production solution [1]. Ammonia can be used as fuel in several technologies, including internal combustion engines, turbines and different

* *Corresponding author.*
E-mail addresses: giovanni.cinti@unipg.it (G. Cinti), vli@energy.aau.dk (V. Liso), ssa@energy.aau.dk (S.S. Araya).
https://doi.org/10.1016/j.ijhydene.2023.01.008

fuel cell types. One of the most promising solutions in terms of high efficiency and nearly zero emissions is a power plant based on Solid Oxide Fuel Cell (SOFC) technology [2]. In SOFC technology ammonia can be directly decomposed in the anode due to high temperatures and nickel as catalyst [3]. Moreover, the cracking reaction allows to reduce the cooling requirement of the system with beneficial advantages at system level [4]. The operation of SOFC with ammonia is reported in literature on an experimental basis both at single cell and stack level [2,5–8]. Experimental evidence shows that SOFCs can completely decompose ammonia internally with no production of NOx [9,10]. Literature also reports preliminary studies on the degradation of SOFC when operated with ammonia, where no increase in degradation rate was measured but nitridation of materials, mainly anode and interconnects, may cause performance loss in the long term [3]. However, degradation is not in the aim of present study and the focus is on the impact of system design on performance and efficiency.

At system level, only few studies are reported, mainly using a design approach from natural gas fuelled SOFC power plants. One of the first model presented in literature in reported in Ref. [11]. Their study was a simple but complete analysis of the SOFC operation with NH_3 as a fuel. The study reports the values obtained from single cell experimental study and illustrates the system design that was modelled. The paper also reports a second design with an improved cathode design strategy aimed at reducing the size of inlet air heat exchanger. This latter part of the study is only introduced in the referred study, and it is more thoroughly investigated and integrated with the newly proposed concept in the current work.

The recirculation of off gasses in several system designs, including ammonia-fed SOFC system has also been studied in Ref. [12]. Their design integrates the recirculation of anode off gasses of an ammonia-fed SOFC at high temperature instead of directly feeding the afterburner. They studied at fuel utilization factor (*Uf*) values of 0.7 and 0.8, and since the concentration of hydrogen in wet off gasses is very low, the recirculation causes a decrease in cell voltage, and consequently in system efficiency. Net efficiency of 51% is calculated with SOFC operating at 750 °C and at a power density of 0.12 W cm^{-2} (calculated from data). Recirculation of off-gasses is a well known strategy in literature that is used to increase efficiency. However, literature studies mainly focus on natural gas and hydrogen fuelled systems [13,14]. Another system based on SOFC and ammonia was also presented in Ref. [15], where steam is added in the anode flow gasses with subsequent strong decrease in performances. In Refs. [16,17], hydrogen is recovered from anode off gasses with a palladium based membrane. In these studies, the aim of the system is the combined production of heat, hydrogen and power, and power production is not optimized. In Ref. [18] the first study with no after burner in the system using a different type of SOFC (so called H–SOFC) has been reported. In our previous studies we evaluated two ammonia-SOFC system designs [4,19]. In the first study [4], the system design includes two heat exchangers for each electrode (one for high and one for low temperature) and an afterburner in the middle that completes the fuel oxidation. At SOFC operating temperature of 750 °C and U_f value of 0.8, a maximum net efficiency of 66% was obtained at very low power density of 0.09 W cm^{-2} (calculated from data). In the second study [19], an improvement of the model based on new experimental results was presented. The new design integrates the SOFC stack with the after burner, that can be bypassed, and three heat exchangers. When the system operates with U_f value of 0.8 and current density of 0.5 A cm^{-2}, a net efficiency of 52.1% was calculated at power density of 0.36 W cm^{-2}.

Recently, an improved SOFC–NH_3 system configuration with a 100% anode off gas recirculation has been reported in Ref. [20]. In their design, nitrogen is separated from hydrogen with a membrane and a pure hydrogen flow is recirculated in the system and mixed with the inlet ammonia, leading to an efficiency increases from 60% to 72%. The main drawback of such a design is related to the introduction of an expensive and not mature component such a palladium-based membrane.

The study presented in this paper advances the afterburner-less design configuration concept in Ref. [19] with new strategies. The removal of the afterburner is possible, because ammonia is not a carbon-based fuel, and therefore, it is not necessary to complete the oxidation of carbon compounds such as CO for environmental reasons. On the contrary, avoiding any combustion is beneficial from an emission reduction point of view, since anode off gasses are nitrogen-rich, and their high temperature combustion can increase the risk of NOx formation. The drawback for afterburner-less design is that all system temperatures decrease with consequent increase of heat exchanger surface areas as previously reported in Ref. [19]. Moreover, without the afterburner, system off gasses still contain hydrogen since the SOFC fuel utilization is lower than unity. Therefore, steam should be condensed and separated, so that the off gasses become a mixture of only nitrogen and hydrogen that can then be fed directly to the SOFC stack for additional power production or to a new stack in the so called cascade configuration [21].

The aim of this paper is to design, model and study an improved ammonia-SOFC system. The novelty of this study is related to the application of cascading and off-gases use in ammonia fuelled SOFC power systems. The use of ammonia introduces new interesting aspects related to thermal balance, hydrogen dilution and oxygen flow management. The strategies studied in the current work are: two cathodes in series (Design A), off-gas recirculation (Design B), stack cascading (Design C). All these solutions are well known in literature for SOFC system design but the new application with ammonia opens to new strategies that deserve a deeper investigation. The objectives of the new design configurations are.

- to further study the design strategy reported in literature [11], where the power rate is divided into two stacks with anode gas provided in parallel and cathode air delivered in series, and no afterburner is implemented (*Design A* in this study);
- to evaluate strategies that increase system fuel utilization using the hydrogen flow rate still present in the off gasses. In particular two strategies are identified: anodic off gasses recirculation (*Design B*) and the introduction of stack

cascading: additional SOFC stack/s operating with the anode exhausts obtaining the repowering of the system (*Design C*);

The three system designs are studied focusing on two main parameters: net system electrical efficiency and heat exchanger surface area. The integration of the different strategies is also considered and studied to identify the best design solution.

Methodology

System design

The aim of this study is to develop an improved configuration for a SOFC system fuelled with ammonia. The model of the SOFC unit is based on a regression study of the data available in literature. This type of model is coherent with the aim of this study, which is not to develop a unit model but to optimize the system design. Further studies may require an electrochemical model.

The SOFC power systems were designed and modelled with a calculation spreadsheet and a code developed using Excel macros, where a data with fluid thermophysical properties was implemented based on Janaf tables [22]. A zero-dimensional model was implemented for all components and thermodynamic energy balance was calculated based on design parameters. The SOFC stack was modelled starting from the voltage calculation, V [V] obtained from reference experimental results as function of current density, J [A cm^{-2}], fuel utilization, U_f, and ammonia concentration, X_{NH3}, [19]. Once U_f and J are fixed, inlet gas flow can be calculated as follows:

$$\dot{n}_{H_2 eq} = \frac{J}{2 \times F \times U_f} \tag{1}$$

where F is Faraday's constant [96,485 C mol^{-1}] and $\dot{n}_{H_2 eq}$ [mol s^{-1}] is the specific hydrogen equivalent molar flow rate per unit area defined as:

$$\dot{n}_{H_2 eq} = \dot{n}_{a,H_2} + \frac{3}{2}\dot{n}_{a,NH_3} \tag{2}$$

where $\dot{n}_{a,H_2}$ [mol s^{-1} cm^{-2}] and $\dot{n}_{a,NH_3}$ [mol $s^{-1}cm^{-2}$] are the hydrogen and ammonia specific molar flow rates entering the anode. The energy and mole balance of the stack are calculated by considering (i) the complete chemical decomposition of ammonia in the anode, (ii) constant heat losses in the stack and (iii) the cathode flow rate calculated to maintain stack temperature at design conditions. The cathode flow rate is obtained by considering the average between inlet and outlet temperatures of both anode and cathode as the stack operating temperature and fixing the difference between the inlet and outlet temperature (ΔT) to 100 °C for both electrodes. The latter is required to reduce thermal stress to the stack. The combination of the two requirements brings to an inlet temperature of −50 °C and +50 °C compared to the operating temperature for inlet and outlet gas flow rates, respectively. However, for multi-stacks configuration the ΔT of 100 °C is the upper limit for the additional stacks and only lower values are accepted when designing the second and third stacks. Once cathode flow rate is calculated, it is possible to derive the utilization of oxygen (Uox) defined as follows:

$$U_{ox} = \frac{J}{4 \times F \times \dot{n}_{c,O_2}} \tag{3}$$

where $\dot{n}_{a,O_2}$ [mol $s^{-1}cm^{-2}$] is the area specific cathodic oxygen molar flow rate. The heat exchangers energy balance is calculated considering the heat balance and with a constant heat transfer efficiency for all components. The model also calculates the heat exchanger surface area, A_{HE} [cm^2_{HE} cm^{-2}] obtained as follows:

$$A_{HE} = \frac{Q_{HE}}{LMTD \times U} \tag{4}$$

where Q_{HE} is the exchanged thermal power, *LMTD* is the logarithmic mean temperature difference and *U* is the heat exchange coefficient fixed at 30 W m^{-2} K^{-1}. Total specific surface area of heat exchangers of the system, A_{THE} [cm^2_{HE} cm^{-2}], is defined as follows:

$$A_{THE} = \sum A_{HEi} \tag{5}$$

Finally, the specific gas blowers power consumption, P_B [W cm^{-2}], was calculated as follows:

$$P_B = \frac{\dot{m}_g \times C_p \times \Delta T}{\eta_B} \tag{6}$$

where $\dot{m}_g$ [mol $s^{-1}cm^{-2}$] is the area specific blower gas mass flow rate, C_p [J K^{-1}] is the gas heat capacity at constant pressure, ΔT [K] is inlet-outlet temperature difference and η_B is the isentropic efficiency of the blower. Temperatures were calculated using blower isentropic adiabatic equation:

$$T_{out} = T_{in} \times \beta^{\frac{k-1}{k}} \tag{7}$$

where T_{in} [K] and T_{out} [K] are inlet and outlet temperature respectively, β is the pressure ratio and k is the adiabatic gas coefficient. Note that to keep the model independent from the power, all dimensional parameter (gas flow rate, power, heat, current, heat exchanger area) were calculated per unit of fuel cell stack active area. In the case of multi-stack design the normalization is done with the total active area of all stacks. This is useful when comparing configurations with different fuel cell stack sizes or different number of stacks, as is the case in the current work.

The system net efficiency is calculated as follows:

$$\eta_{net} = \frac{V \times J}{LHV_{NH_3} \times \dot{n}_{NH_3}} \tag{8}$$

where $\dot{n}_{NH_3}$ [mol $s^{-1}cm^{-2}$] is the specific inlet ammonia flow rate and LHV_{NH_3} [J mol^{-1}] is ammonia Lower Heating Value. The gross efficiency is calculated using the following equation:

$$\eta_{gross} = \frac{\eta_i \times V \times J - \sum P_{Bi}}{LHV_{NH_3} \times \dot{n}_{NH_3}} \tag{9}$$

where η_i is inverter efficiency and $\sum P_{Bi}$ is the sum of all blowers' area specific power consumption. All the models presented in this study follow common design strategies. The thermal energy balance of the SOFC is obtained varying the

cathode flow rate, and consequently, the utilization of oxygen. Ammonia is stored in pressurized conditions and the blower is not necessary at fuel inlet. Ammonia does not undergo any decomposition before entering the SOFC stack. A pre-cracking reactor was not considered and the ammonia decomposition occurs directly inside the anode. Finally, the use of after-burners was avoided to reduce the possible NOx formation due to high N_2 content in anode off gases and due to no obligation to oxidize the remaining fuel thanks to the carbon-free nature of NH_3 fuel.

In all simulations the fuel utilization and the current density were kept constant at 0.8 and 0.5 A cm^{-2}, respectively. These values are considered a good trade-off between efficiency and power density. Stack temperature was fixed to 750 °C according to state-of-the-art value. The constant parameters used in the current work are reported in Table 1.

Table 1 – Constant design parameters used in the model simulations.

Parameter	Value	Reference
Stack fuel utilization (U_f)	0.8	
Stack current density (J)	0.5 A cm^{-2}	[13]
Ambient inlet air conditions	T = 293.15 K, P = 1 bar	
Average SOFC temperature (T_{avg})	750 °C	[13, 23]
Heat exchanger efficiency (η_{HE})	0.9	[23]
SOFC thermal losses (η_{Qloss})	0.05	[19]
Cathode pressure drops (cathodic blower design) (ΔP_{cat})	100 mbar	[13]
Anodic pressure drops (recirculation blower design) (ΔP_{and})	25 mbar	[13]
Blowers' isentropic efficiency (η_B)	0.85	[20]
Inverter efficiency (η_{inv})	0.9	[13]

The three identified system configurations are described below.

Design A: *System design with power rate*

In the first design configuration, two different SOFC units are considered and the system is operated at different power rates. Power rate (PR) is defined as the ratio between the power of the single stack and the total sum of the power of all the stacks $PR = \frac{P_{stack}}{P_{tot}}$. For *Design A*, where only two stacks are involved $PR = \frac{P_{SOFC1}}{P_{SOFC1}+P_{SOFC2}}$. Fig. 1 shows the system design with the introduction of the first system improvement (*Design A*).

The design is based on what is already presented in Ref. [11], where two stacks are connected in parallel for what concerns anodic gas flows, while the cathodic gas flows are delivered in series with the enrichment of fresh air flow between the two units. The fresh flow is introduced to reduce the inlet temperature of the anodic mixture of the second stack. At system level, this strategy allows to reduce the air flow rate that must be preheated in the cathodic heat exchanger. Compared to what is already described in literature, this system design does not consider the post combustion of anode exhausts in an after burner to reduce system components and to eliminate the risk of NOx formation. The final result of this new design is a power rate split between the two stacks. To operate the two stacks, it is necessary to distribute both anodic and cathodic gas flow introducing splitting valves. Ammonia is preheated in the heat exchanger called anodic recuperator that can operate also as NH_3 cracking reactor, depending on the design strategies. The fuel is divided in a splitter (S1) feeding the two anodes of the stacks with the same gas composition but different flow rates, depending on the power rate. From the anodic gas point of view, the two stacks are in parallel. Stack anode exhausts are joined in the

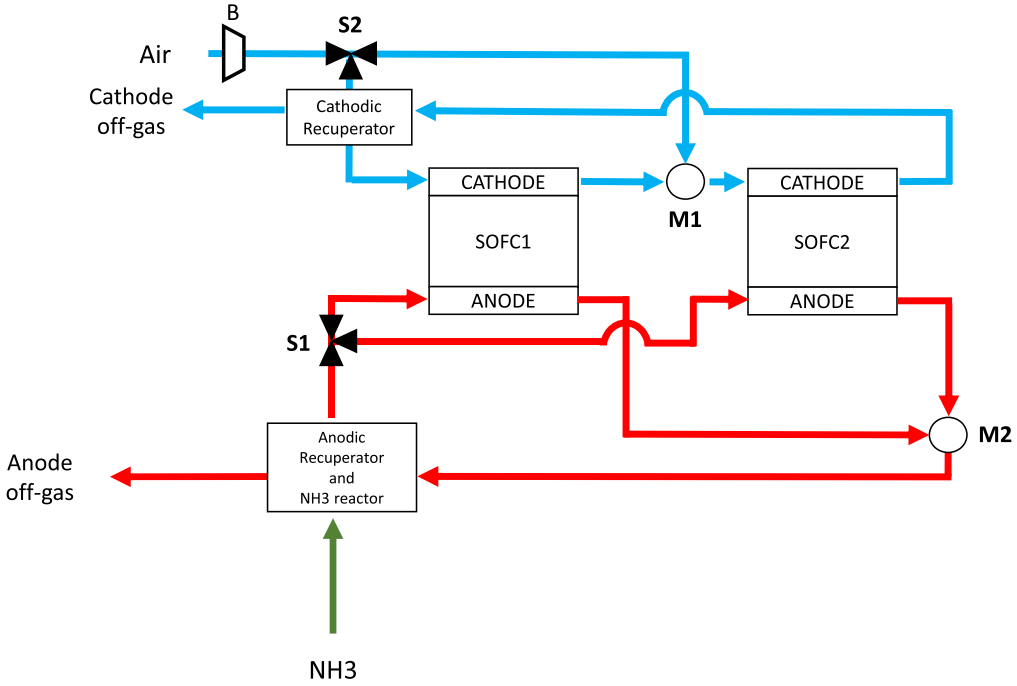

Fig. 1 – System design with power rate (*Design A*).

mixer M2, and from M2 the gases flows through the anodic recuperator to provide the heat to the inlet fuel. Anode off-gasses are then flashed into the atmosphere. Note that since no afterburner is introduced, anode off-gases still contain the amount of hydrogen that did not react in the stacks. Air is introduced into the system at atmospheric conditions using the blower B. The air flow is separated in the cathodic splitter (S2). These units split the amount of air flow that will pass through the heat exchanger to the first stack, from the air necessary to reduce cathodic mixture temperature between the two stacks. While the air flow directed to the first stack is designed to reach thermal balance of the stack, the air flow separated and introduced in the mixer M1 is calculated to decrease temperature of first stack cathodic exhausts to the inlet temperature of second stack. For the second stack the inlet temperature is calculated, so that an average temperature of 750 °C between cathodic inlet and outlet is reached. The cathodic gas flows from the second stack are cooled in the cathodic heat exchanger, where heat is transferred to the inlet air of the first stack.

Design B: *System design with power rate and anode recirculation*

This design is an improvement of first design with the introduction of anode recirculation. Since both stacks operate with a utilization of fuel lower than one, off gasses contain a flow rate of hydrogen that can be recirculated. In *Design B*, part of the off gasses flow rate is separated after the anodic recuperator in the anode off gas recirculation (AOR) valve, as shown in Fig. 2. The composition of the off gasses is mainly steam, nitrogen and hydrogen, before the steam is separated in a condenser (COND). Then a recirculation blower (RB) allows to recirculate the gasses. Recirculated flow rate is mixed with the fresh ammonia inlet in the mixer M3. The recirculated gas mixture is composed of hydrogen and nitrogen, a fuel and an inert. This means that the new fuel mixture entering the anodic recuperator is a mixture of ammonia, nitrogen and hydrogen. Depending on the equilibrium conditions, the new mixture entering the SOFC stacks could vary in concentrations. The recirculation rate (RR) is defined as the ratio between the recirculated flow rate and the total flow rate entering the AOR valve.

Design C: System design with power rate, anode recirculation and repowering

Another strategy to increase system efficiency is to introduce a third stack in the system design, thereby obtaining a repowering of the power plant. This solution (*Design C*) is represented in Fig. 3. The scheme reported in the figure integrates both the recirculation and the repowering solutions. After the condenser, a second separation splitter is introduced to get a re-power of the system (S4) that separates the condensate and sends the remaining gases to a third stack SOFC3. The repowering parameter (RP) is defined as the ratio between the flow rate that reaches the third stack and the flow rate entering the splitter S4. Before entering the stack, the mixture is heated up to anode inlet temperature in a second anodic recuperator. The latter is fed, in the hot side, by the anodic off gasses of the stack before exiting the system via the mixer M4. The cathode of the third stack is fed with air from the splitter S2. In this design, like in the power rate design (*Design A*), the cathodic flow is preheated in the mixer M5 using hot mixture exiting the second stack cathode. Fresh air is necessary to reduce the third stack's inlet temperature and to introduce additional oxygen flow rate. Repowering ratio is controlled with the RP or with the combination of AOR and RP.

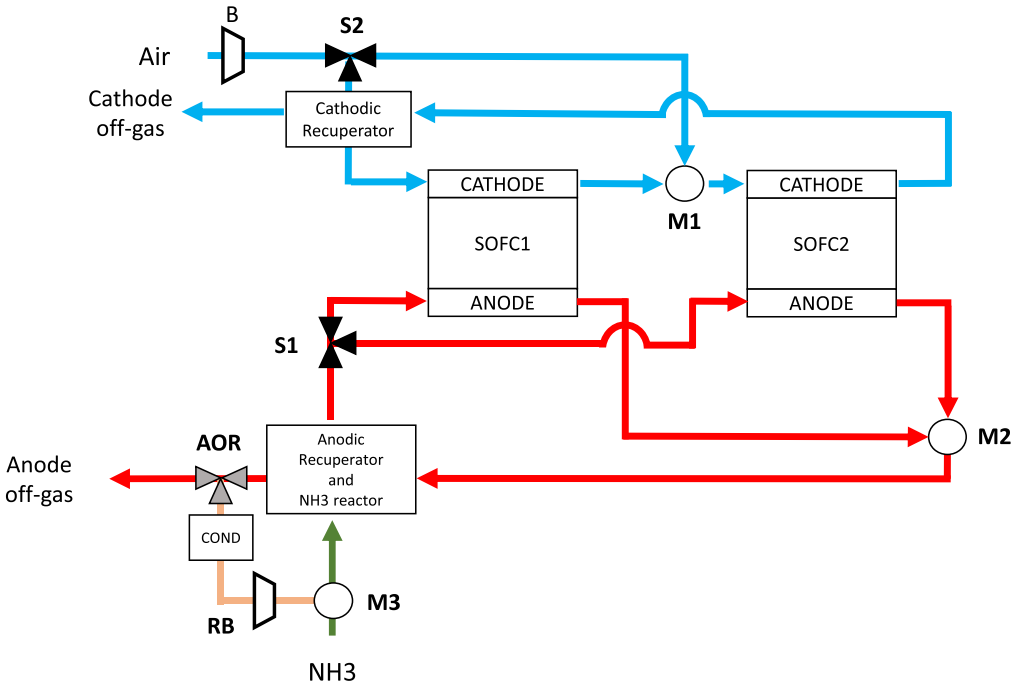

Fig. 2 – System design with power rate and anode recirculation (*Design B*).

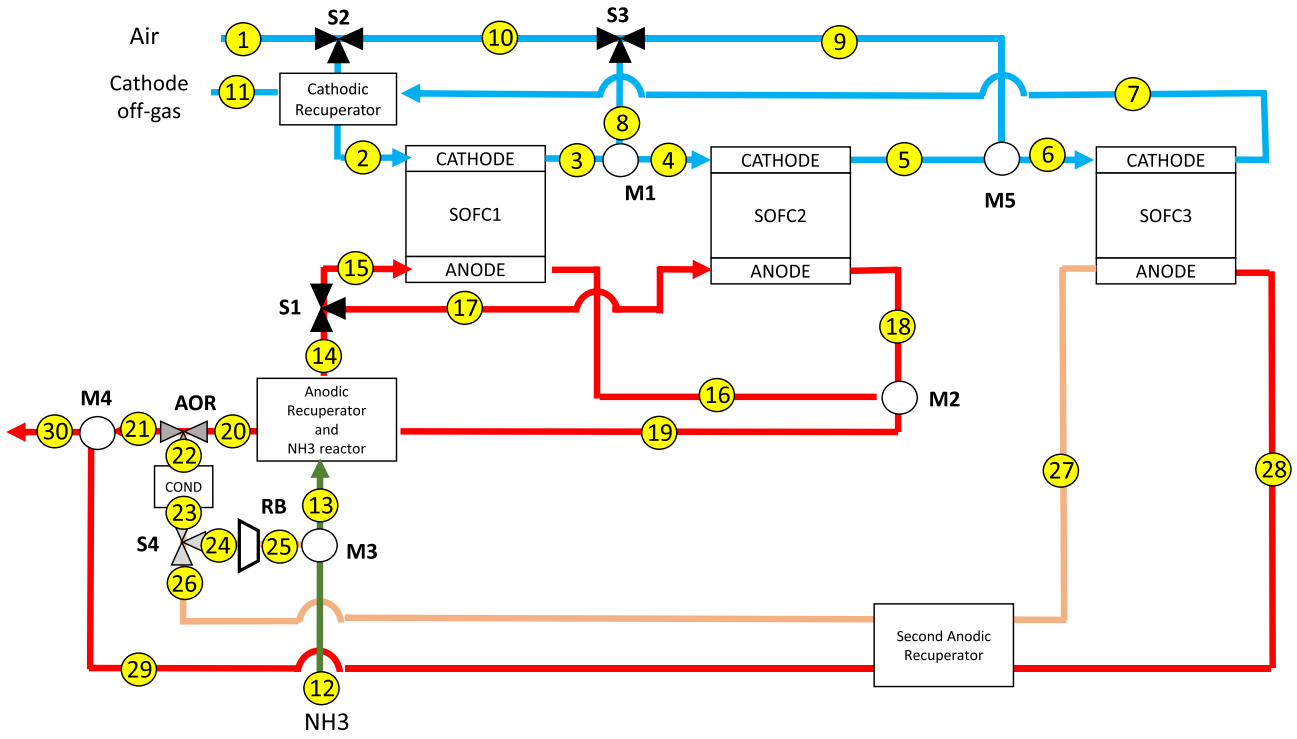

Fig. 3 – System design with power rate, anode recirculation and repowering (*Design C*).

The cathode flow is regulated accordingly in S2 so that the third stack operates in the required thermal conditions. It is worth highlighting that this design does not require additional power for blowers in terms of pressure drops since the cathode pressure drop is the same due to the parallel configuration and in the anode side the ammonia storage pressure conditions allow to add components without additional pressure requirements.

Results

Results of the system study are here below reported for each of the three studied configurations.

Design A

The system was studied by varying the power rate from 1, where only one stack operates, to 0.5, where the power is equally distributed between the two stacks. Fig. 4 shows the results of the variation of oxygen utilization for both the first stack (U_{ox1}) and the second stack (U_{ox2}) as function of power rate. While U_{ox1} is at a constant value of 0.2, i.e., the first stack operates always at the same conditions,U_{ox2} increases up to a value of 0.22 when PR is reduced to 0.5. The main result of *Design A* strategy is the reduction of air flow rate, also reported in Fig. 4. When the power is equally distributed between the two stacks (PR = 0.5), air flow rate is reduced by 43%, which leads to reduction in the power consumption of blower B.

Both parameters are plotted in Fig. 5 as function of PR. The gas flow rate entering the cathodic recuperator (CR) decreases linearly with the decrease in PR value, achieving 50% of gas flow reduction for PR = 0.5. The off gas air temperature and the inlet-outlet gas temperature of the second stack are also shown in the Figure. Owing to the introduction of the power rate, off gas temperature rises to 93 °C for PR = 0.5. Such value allows to achieve feasible value for the cathodic heat exchanger temperature levels. On the other hand, PR = 0.5 is a minimum value of power rate for the stack temperature difference limits, defined by ΔT SOFC2. As reported in the graph, such difference increases linearly when power is rated to the second stack (PR value approaching 0.5). The limit value of 100 °C is achieved for PR values smaller than 0.5, which is determined by both U_{ox2} (see Fig. 4) and ΔT SOFC2 as design limits.

The variations of net and gross efficiencies as function of power rate are shown in Fig. 6. Since both stacks always operate at the same conditions of U_f value and power density, the gross efficiency is constant at 57%. When the second stack is introduced, the net efficiency increases from 50 to 53%. As

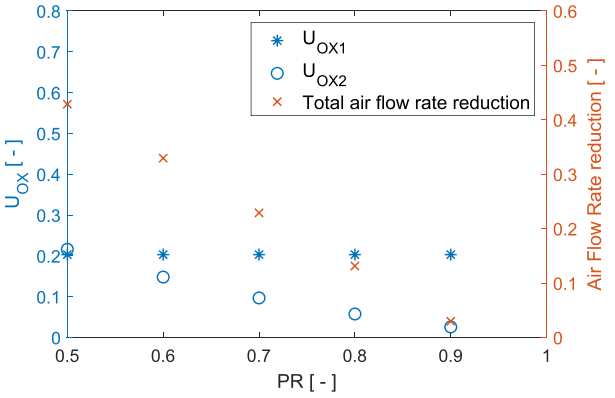

Fig. 4 – U_{ox} and Air flow rate reduction as function of PR.

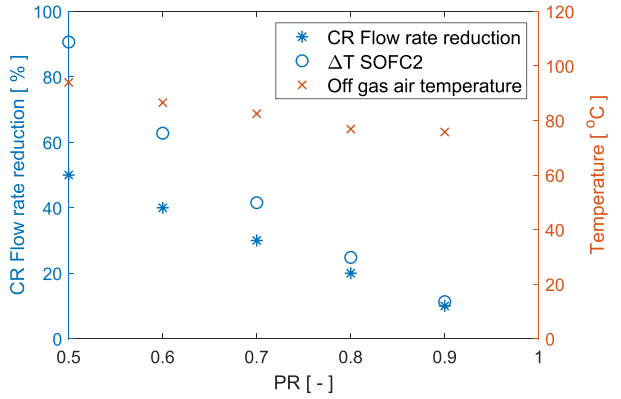

Fig. 5 – Variation of and CR flow rate reduction, off gas temperature and Δ T SOFC2 as function of PR.

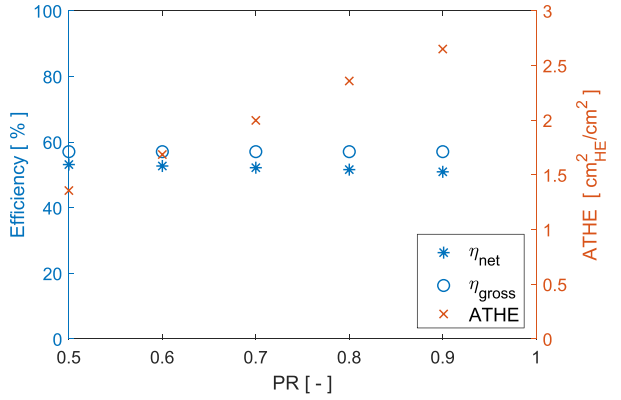

Fig. 6 – Net and gross system efficiency at PR variation for *Design A*.

reported in equations (8) and (9), the difference between the two efficiencies is related to the inverter efficiency and the energy consumption of blowers. The latter is reduced in *Design A* since air flow rate entering the system is lower and, consequently, net efficiency increases. Fig. 6 also shows the total area of the heat exchanger (ATHE). It must be noted that this parameter is measured as heat exchanger surface area per unit area of fuel cell stack. The value of ATHE, not available for PR = 1 due to the already mentioned temperature issues, decreases down to 1.36 cm^2_{HE} cm^{-2} with decreasing air flow rate. Finally, the power density of each stack is 0.39 W cm^{-2}. This value does not depend on the power rate since operating conditions in terms of current density and fuel utilization are the same for both stacks.

Design B

To evaluate the effect of recirculation on system performances, recirculation rate (RR) was varied from 0 (no recirculation) to 0.8 with a step of 0.2. A complete recirculation (RR = 1) it is not possible since nitrogen is recirculated with hydrogen and must be removed from the system. The system was operated with the optimized power rate of 0.5 (see *Design A* study). Gas recycling brings to a modification of anode mixture as reported in Fig. 7, i.e., causes dilution of inlet

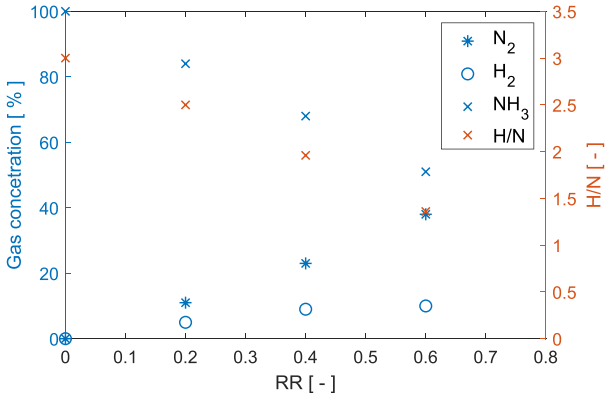

Fig. 7 – Utilization factors of *Design B* as function of RR.

ammonia with mixture of H_2 and N_2. The H/N ratio that accounts the anode inlet operating conditions in terms of dilution factor is shown in Fig. 7. When the system operates with no recirculation, H/N ration is 3, that is the same value of pure ammonia. Recirculation rate reduces this ratio down to 0.75 in case the system operates with RR equal to 0.8.

Fig. 8 shows utilization factors and efficiencies as function of RR for *Design B*. Utilization of oxygen for both stacks remain

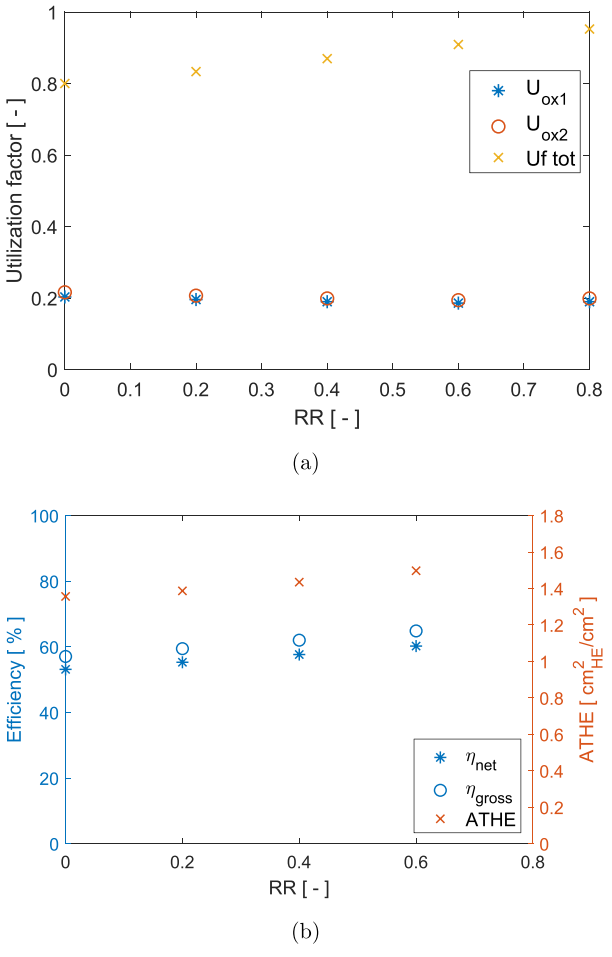

Fig. 8 – Parametric changes for *Design B* at varying RR (a) Utilization factors (b) and net, gross system efficiency and A_{THE}.

in the 0.2 range value with minimum variations. Fig. 8(a) also shows the total U_f value, where the stack U_f is a design parameter set to 0.8. As expected, recirculation rate allows to increase the total fuel utilization up to 0.95 for a RR value of 0.8. As can be seen in Fig. 8(b), the increase in recirculation rate improves both grosse and net efficiencies linearly up to values of 0.68 and 0.63, respectively. The contribution of the higher ancillary power absorbance due to the recirculation blower does not emerge from the efficiency analysis. This is caused by the low values of recirculation rate compared to that of the air blower. Moreover, Fig. 8(b) shows the total area of the heat exchanger, where an increase in RR leads to increase in gas flow rates and decrease in temperatures. This in turn causes an increase in the total heat exchanger surface area that reaches a value of 1.64 cm^2_{HE} cm^{-2} for RR = 0.8.

Design C

To evaluate the effect of repowering on system performances, repower rate (RP) was varied from 0 (no repowering) to 1 (full repowering) with a step of 0.2. The system was operated with the optimized power rate of 0.5 (see *Design A* study) and no recirculation (RR = 0). The third stack always operates with dry off gasses, whose composition is a function of the U_f values of the first two stacks. Once U_f is fixed to 0.8, concentration of H_2 and N_2 in the third stack are 37.5% and 62.5%, respectively. The utilization factor and the power rates at varying RP are shown in Fig. 9. The results in Fig. 9(a) show that the oxidant utilization factors remain constant for the first two stacks at 0.2 and 0.22, respectively. Whereas for the third stack, U_{ox3}, the values increase with increasing RP values, up to 0.09. The cathodic flow rate of the third stack is a mixture of the fresh fuel and the cathodic off gasses of the second stack, the oxygen utilization of third stack increases with increasing RP. This results in a lower oxygen utilization of the third stack compared to the previous two. The total U_f reaches values up to 0.96, which is possible since unused hydrogen from the first two stacks is fed to the third one.

The reason for the variation in U_{ox3} can be seen in Fig. 9(b), where the power rate of the three stacks are shown. The first and second fuel cell stacks (SOFC1 and SOFC2 in Fig. 3) have the same power rate (PR1 = PR2). However, the power rates of the first two stacks decrease from 0.5 to 0.42 when RP increases 0 to 1. This is a consequence of the operation of stack 3, whose power rate (PR3) increases from 0 to 0.18.

An additional consequence of repowering is reported in Fig. 10(a), where CR and total air flow rate reduction is reported as a function of RP. Compared to the design without repowering, the distribution of power among the three stacks allows to reduce both the flow rate in the cathodic recuperator and the total air flow rate by 58% and 48%, respectively. CR flow rate is important since it is directly related to CR size and relative cost, while total air flow rate impacts system design as it is the main parameter used to design air blower and its relative power consumption. Gross and net efficiency as function of RP are reported in Fig. 10(b), where they increase up to 0.68 and 0.64, respectively. Fig. 10(b) shows A_{THE} values, where the distribution of the power between the stacks allows

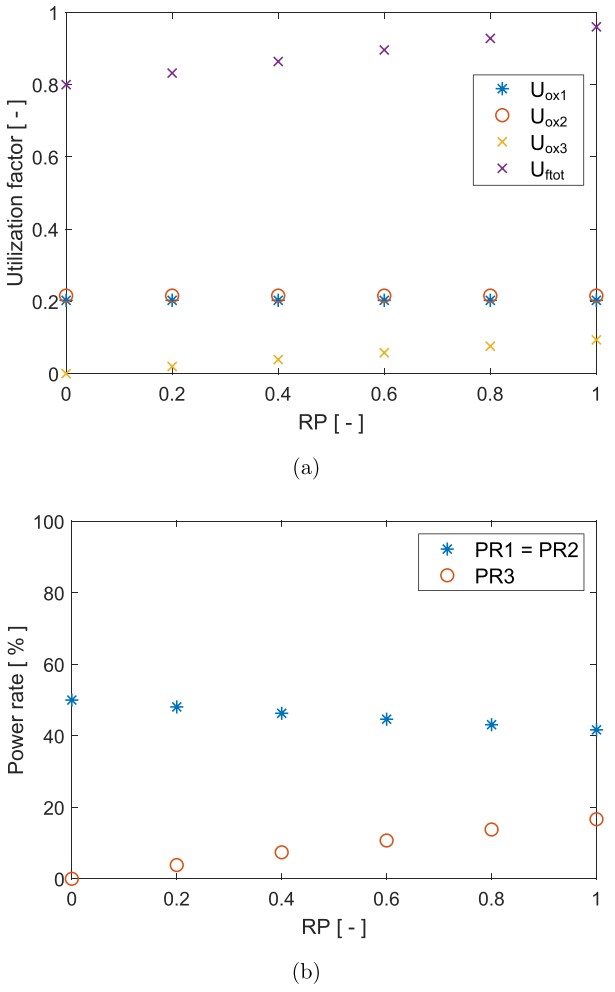

Fig. 9 – Parametric changes for *Design C* at varying RP (a) utilization factors and (b) power rate.

to reduce the value of this parameter even with the increasing contribution of the second anodic recuperator. The minimum value of A_{THE} is obtained at RP = 1 and reaches a value of 0.87 cm^2_{HE} cm^{-2}.

Discussion

All the proposed designs strategies improved the system both in terms of efficiency and lower total heat exchanger surface, compared to a single stack configuration. While the power rate strategy is considered an efficient solution that can be implemented in future SOFC–NH_3 systems, recycling and repowering are considered alternative solutions to reduce energy losses and increase efficiency. An integration of both solutions is possible with RR of 0.8 and RP of 1, while PR was kept at the optimal value of 0.5. The main results of this final case are reported in Table 2, where a total fuel utilization of 0.99 and net electrical efficiency of 66% can be achieved, a significant increase from the 52.1% reported at similar operating conditions in Ref. [19]. The temperatures and compositions of the flows for this design are provided in Table 3 and

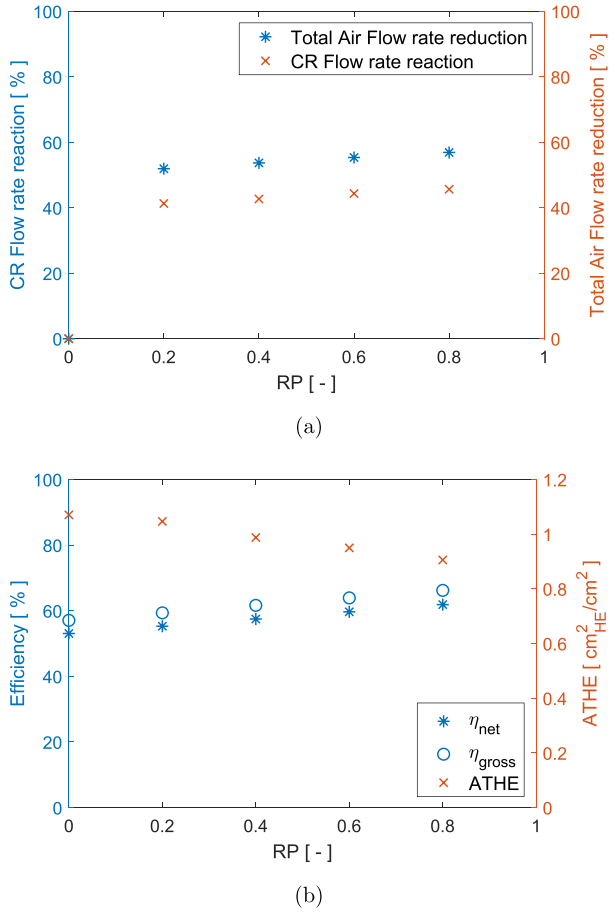

Fig. 10 – Parametric changes for *Design C* at varying RP (a) total air flow rate and CR flow rate reduction and (b) System efficiencies.

Table 4, respectively, where both tables use the same labels of the pipes as in Fig. 3. In the final system it is possible to define the power rate of each stack (PR1, PR2 and PR3) as the ratio between the power of relative stack and the total power of the system, and therefore, PR1 and PR2 are 48% each and the third stack covers the remaining 4% of the power. It is important to underline that the power density, *Pd*, of the system is always the same at 0.39 W cm^{-2}, since all the stacks operate with the same current density of 0.5 A cm^{-2} and the same fuel utilization of 0.8. However, with this optimization the RR is high

Table 2 – Design parameters for optimized efficiency.

Parameter	Value
U_{ox1}	0.19
U_{ox2}	0.2
U_{ox3}	0.02
U_{ftot}	0.99
PR_1	0.48
PR_2	0.48
PR_3	0.04
Pd [W cm^{-2}]	0.39 W cm^{-2}
η_{net}	0.66
η_{gross}	0.71
A_{THE} [cm^2_{HE} cm^{-2}]	1.34

Table 3 – Composition of flows for *Design C*. The number in brackets indicate the pipe numbers in Fig. 3.

Pipe nr.	1	2	3	4	5	6	7	8	9	10	11	12	13	14	15	16	17	18	19	20	21	22	23	24	25	26	27	28	29	30
T [°C]	20	700	800	705	796.1	780	790.5	20	20	20	113.5	20	20	700	700	800	700	796.1	798	189.6	189.6	189.6	20	20	20	20	700	790.5	62.4	62.2

Table 4 – Composition of flows for *Design C*. The numbers in brackets indicate the pipe numbers in Fig. 3.

Composition	H_2O [%]	N_2 [%]	H_2 [%]	NH_3 [%]	O_2 [%]
Air (1, 2, 11, 12)	0	79	0	0	21
$SOFC_1$ cathode out (2, 3)	0	82.3	0	0	17.7
$SOFC_2$ cathode in (4)	0	81.9	0	0	18.1
$SOFC_2$ cathode out (5)	0	84.9	0	0	15.1
$SOFC_3$ cathode in (6)	0	84.8	0	0	15.2
$SOFC_3$ cathode out (7)	0	85	0	0	15
$SOFC_3$ cathode off-gas (7, 11)	0	85	0	0	15
NH_3 in (12)	0	0	0	100	0
NH_3 decomposition (14,15,17)	0	60.9	8.7	30.4	0
$SOFC_1$ anode out (16, 18)	33.3	58.3	8.3	0	0
Anode recuperator mix (19, 20, 21, 22)	33.3	58.3	8.3	0	0
Ary gases recirculation (23,24,25,26,27)	0	87.5	12.5	0	0
$SOFC_3$ anode out (28,29)	10	87.5	2.5	0	0
System off gasses (30)	10	87.5	2.5	0	0

Table 5 – Parameters of high efficiency design and low A_{THE} design. Reference design is defined as *Design A* with PR = 0.

Parameter	Reference design	High efficiency design	Low A_{THE} design
PR	1	0.5	0.5
RR	0	0.8	0
RP	0	1	1
Pd [W cm^{-2}]	0.39	0.39	0.39
η_{net}	0.5	0.66	0.64
η_{gross}	0.57	0.71	0.68
A_{THE} [cm^2_{HE} cm^{-2}]	> 2.65	1.34	0.87
Total power [kW]	100	100	100
Total SOFC active area [m^2]	25.6	25.6	25.6
Total A_{THE} [m^2_{HE}]	> 67.84	34.25	22.21

and A_{THE} reaches a value of 1.34 cm^2_{HE} cm^{-2}, which is 54% more than the minimum area obtained by optimizing for heat exchanger surface area.

All strategies presented in this study require the increase in the number of stacks. This aspect could be considered as significant complexity compared to the mentioned advantages. However, SOFC technology is based on a modular design and, to reach high powers, more stacks are required even in the standard system design configurations. From this work, it is possible to identify two optimal conditions defined as high efficiency design and low A_{THE}, reported in Table 5, where total power and total SOFC area are also calculated for a 100 kW system. The table also reports the base case where none of the three strategies is implemented. Since *Design A* does not achieve the thermal energy balance for all heat exchangers, the data of A_{THE} have to be considered higher of the closer one (case PR = 0.8).

The data reported in Table 5 shows that the low A_{THE} design seems optimal since the loss of net efficiency compared to the high efficiency design is very low, 3.1%, compared to the decrease of A_{THE}, 35.1%. Therefore, the final design decision is a trade-off between capital investments and operative costs in terms of fuel consumption.

Conclusion

The use of ammonia in SOFC systems has a significant impact on traditional system design. In this study three design strategies are introduced and evaluated in terms energy efficiency and impact on the balance of plant components. The main objective was to reduce the surface area of the heat exchangers, and consequently, their relative cost. It was found that with an integration of the three solutions, it is possible to achieve an increase in net efficiency from 52.1% to 66% and a reduction in heat exchanger surface area of 67% compared to the reference design that does not consider any of the proposed design strategies. The power rating strategy allows to halve the heat exchanger surface area and to operate the system without an afterburner. The anode off gas recirculation strategy increases efficiency but with an increase in heat exchanger surface. Finally, the re-powering solution has the advantage of both increasing the efficiency and reducing the surface area of the heat exchangers. Therefore, the best solution is with repowering and low A_{THE} optimization, which allows to increase net efficiency by 28% and to reduce the total surface area of heat exchanger by 35.1%. It can be concluded that the proposed solution improves the ammonia-fed SOFC system design both in terms of efficiency increase and lower heat exchanger surface area. This is done without necessarily increasing the complexity of the system since SOFC technology usually requires a modular approach that involves different SOFC units.

Declaration of competing interest

The authors declare that they have no known competing financial interests or personal relationships that could have appeared to influence the work reported in this paper.

Nomenclature

β	Pressure ratio
ΔP_{and}	Anodic pressure drop
ΔP_{cat}	Cathode pressure drop

η_B	Blowers' isentropic efficiency
η_{HE}	Heat exchanger efficiency
η_{inv}	Inverter efficiency
η_{Qloss}	SOFC thermal losses
A_{HE}	Heat exchanger area
A_{THE}	Total heat exchangers area
C_p	heat capacity at constant pressure
F	Faraday's constant
J	Current density
LHV	Lower Heating Value
$LMTD$	logarithmic mean temperature difference
P_B	Specific gas blower power consumption
Pd	Power density
T_{avg}	Average SOFC stack temperature
T_{in}	SOFC stack inlet temperature
T_{out}	SOFC stack outlet temperature
U	Heat exchange coefficient
U_f	Utilization of fuel
U_{ox}	Utilization of oxygen
V	Voltage
AOR	Anode off gas recirculation
COND	Condenser
CR	Cathodic recuperator
M	Mixer
PR	Power rate
RB	Recirculation blower
RP	Repower rate
RPS	Repower rate of the system
RR	Recirculation rate
S	Splitter
SOFC	Solid Oxide Fuel Cell

REFERENCES

[1] Valera-Medina A, Xiao H, Owen-Jones M, David WI, Bowen PJ. Ammonia for power. Prog Energy Combust Sci 2018;69:63–102. https://doi.org/10.1016/J.PECS.2018.07.001.

[2] Rathore SS, Biswas S, Fini D, Kulkarni AP, Giddey S. Direct ammonia solid-oxide fuel cells: a review of progress and prospects. Int J Hydrogen Energy 2021;46:35365–84. https://doi.org/10.1016/J.IJHYDENE.2021.08.092.

[3] Kishimoto M, Furukawa N, Kume T, Iwai H, Yoshida H. Formulation of ammonia decomposition rate in ni-ysz anode of solid oxide fuel cells. Int J Hydrogen Energy 2017;42:2370–80. https://doi.org/10.1016/J.IJHYDENE.2016.11.183.

[4] Cinti G, Discepoli G, Sisani E, Desideri U. Sofc operating with ammonia: stack test and system analysis. Int J Hydrogen Energy 2016;41. https://doi.org/10.1016/j.ijhydene.2016.06.070.

[5] Wan Z, Tao Y, Shao J, Zhang Y, You H. Ammonia as an effective hydrogen carrier and a clean fuel for solid oxide fuel cells. Energy Convers Manag 2021;228. https://doi.org/10.1016/j.enconman.2020.113729.

[6] Siddiqui O, Dincer I. A review and comparative assessment of direct ammonia fuel cells. Therm Sci Eng Prog 2018;5. https://doi.org/10.1016/j.tsep.2018.02.011.

[7] Afif A, Radenahmad N, Cheok Q, Shams S, Kim JH, Azad AK. Ammonia-fed fuel cells: a comprehensive review. Renew Sustain Energy Rev 2016;60:822–35. https://doi.org/10.1016/J.RSER.2016.01.120.

[8] Kishimoto M, Muroyama H, Suzuki S, Saito M, Koide T, Takahashi Y, Horiuchi T, Yamasaki H, Matsumoto S, Kubo H, Takahashi N, Okabe A, Ueguchi S, Jun M, Tateno A, Matsuo T, Matsui T, Iwai H, Yoshida H, Eguchi K. Development of 1 kw-class ammonia-fueled solid oxide fuel cell stack. Fuel Cell 2020;20:80–8. https://doi.org/10.1002/FUCE.201900131.

[9] Wojcik A, Middleton H, Damopoulos I, Herle JV. Ammonia as a fuel in solid oxide fuel cells. J Power Sources 2003;118:342–8. https://doi.org/10.1016/S0378-7753(03)00083-1.

[10] Pelletier L, McFarlan A, Maffei N. Ammonia fuel cell using doped barium cerate proton conducting solid electrolytes. J Power Sources 2005;145:262–5. https://doi.org/10.1016/J.JPOWSOUR.2005.02.040.

[11] Dekker NJ, Rietveld G. Highly efficient conversion of ammonia in electricity by solid oxide fuel cells. J Fuel Cell Sci Technol 2006;3. https://doi.org/10.1115/1.2349536.

[12] Rokni M. Addressing fuel recycling in solid oxide fuel cell systems fed by alternative fuels. Energy 2017;137. https://doi.org/10.1016/j.energy.2017.03.082.

[13] Peters R, Deja R, Engelbracht M, Frank M, Nguyen VN, Blum L, Stolten D. Efficiency analysis of a hydrogen-fueled solid oxide fuel cell system with anode off-gas recirculation. J Power Sources 2016;328:105–13. https://doi.org/10.1016/j.jpowsour.2016.08.002.

[14] Liso V, Nielsen MP, Kær SK. Influence of anodic gas recirculation on solid oxide fuel cells in a micro combined heat and power system. Sustain Energy Technol Assessments 2014;8:99–108. https://doi.org/10.1016/j.seta.2014.08.002.

[15] Farhad S, Hamdullahpur F. Conceptual design of a novel ammonia-fuelled portable solid oxide fuel cell system. J Power Sources 2010;195. https://doi.org/10.1016/j.jpowsour.2009.11.115.

[16] Perna A, Minutillo M, Jannelli E, Cigolotti V, Nam SW, Han J. Design and performance assessment of a combined heat, hydrogen and power (chhp) system based on ammonia-fueled sofc. Appl Energy 2018;231. https://doi.org/10.1016/j.apenergy.2018.09.138.

[17] Minutillo M, Perna A, Trolio PD, Micco SD, Jannelli E. Techno-economics of novel refueling stations based on ammonia-to-hydrogen route and sofc technology. Int J Hydrogen Energy 2021;46. https://doi.org/10.1016/j.ijhydene.2020.03.113.

[18] Baniasadi E, Dincer I. Energy and exergy analyses of a combined ammonia-fed solid oxide fuel cell system for vehicular applications. Int J Hydrogen Energy 2011;36. https://doi.org/10.1016/j.ijhydene.2011.04.234.

[19] Barelli L, Bidini G, Cinti G. Operation of a solid oxide fuel cell based power system with ammonia as a fuel: experimental test and system design. Energies 2020;13. https://doi.org/10.3390/en13236173.

[20] Selvam K, Komatsu Y, Sciazko A, Kaneko S, Shikazono N. Thermodynamic analysis of 100% system fuel utilization solid oxide fuel cell (sofc) system fueled with ammonia. Energy Convers Manag 2021;249. https://doi.org/10.1016/j.enconman.2021.114839.

[21] Koo T, Kim YS, Lee D, Yu S, Lee YD. System simulation and exergetic analysis of solid oxide fuel cell power generation system with cascade configuration. Energy 2021;214:119087. https://doi.org/10.1016/j.energy.2020.119087.

[22] Chase M. Nist-janef thermochemical tables. 4th ed. Journal of Physical Chemistry Monograph; 1998.

[23] Barelli L, Bidini G, Cinti G, Ottaviano P. Solid oxide fuel cell systems in hydrogen-based energy storage applications: performance assessment in case of anode recirculation. J Energy Storage 2022;54:105257. https://doi.org/10.1016/j.est.2022.105257.